HEFAT 2007
5th International Conference on Heat Transfer, Fluid Mechanics and Thermodynamics
Sun City, South Africa
Paper number: BT2

THREE-DIMENSIONAL GEOMETRIC OPTIMISATION OF HEAT-GENERATING PLATES COOLED BY FORCED CONVECTION

Bello-Ochende, T*, Dirker, J. and Meyer, J.P.
*Author for correspondence
Department of Mechanical and Aeronautical Engineering,
University of Pretoria,
Pretoria, 0002,
South Africa,
E-mail: tunde.bello-ochende@up.ac.za

ABSTRACT
This paper extends the concept of generating the multi-scale structure for a finite-size flow system to three-dimensional heat-generating plates with maximum heat transfer rate density. The fluid is forced through a given volume containing the heat generating plates by an applied pressure difference (ΔP). The heat-generating plates are arranged in a stack. This work consists of numerical simulation in a large number of flow configurations, one differing slightly from the next to determine the optimum plate spacing and maximum heat transfer rate density. The heat transfer rate density is further increased by inserting smaller three-dimensional plates between the bigger larger plates and optimising the whole structure. The effects of plate thickness and dimensionless pressure drop number on the resulting multi-scale structure are reported. The numerical results are found to be in good agreement with predicted results.

NOMENCLATURE

Be	[-]	Dimensionless pressure number
d	[m]	Spacing between two-dimensional parallel plates
D_0	[m]	Spacing between two plates
D_1	[m]	Spacing between the L_0 and L_1 plates when L_1 plate is inserted
H	[m]	Stack height
k	[W/mK]	Thermal conductivity
L_u	[m]	Length of control volume before the plate
L_0	[m]	Plate length in the flow direction
L_1	[m]	Flow length of the first plate insert
L_d	[m]	Length of control volume after the plate
m	[-]	Number of new inserted plates
n	[-]	Number of plates
P	[N/m^2]	Pressure
Pr	[-]	Prandtl number
Re	[-]	Reynold number
q	[W]	Heat transfer
$\tilde{q}$	[-]	Dimensionless heat transfer, Eq. (13)
t	[m]	Plate thickness
T	[K]	Temperature
T_w	[K]	Temperature
T_∞	[K]	Free-stream temperature
u	[m/s]	Velocity component
v	[m/s]	Velocity component
w	[m/s]	Velocity component
U_∞	[m/s]	Free-stream velocity
W	[m]	Plate breadth
x	[m]	Cartesian axis direction
y	[m]	Cartesian axis direction
z	[m]	Cartesian axis direction

Special characters

α	[m^2/s]	Thermal diffusivity
μ	[kg/s m]	Viscosity
ν	[m^2/s]	Kinematic viscosity
γ	[-]	Convergence criterion
δ	[m]	Boundary layer thickness

Subscripts

d	Downstream
L_0	Length
m	Maximum
opt	Optimum
u	Upstream
$wall,w$	Wall
∞	Free-stream

Superscript

~	Dimensionless

INTRODUCTION
Compactness and miniaturisation are driven by the need to install more and more heat transfer into a given volume. The figure of merit is heat transfer density. A recent trend in heat transfer research has been the focus on the generation of optimal flow architecture, as a mechanism by which the system achieves its maximal density objective under constraints [1]. The strategy is to endow the flow configuration with the freedom to morph, and to examine systematically many of the eligible design configurations. Strategy and systematic search mean that architectural features that have been found to be beneficial in the past can be refined and incorporated into more complex systems of the present. A similar idea has also been pursued and implemented by Dirker et al. [2] in the cooling of power electronics by embedded solids.

One class of flow features that aid the achievement of high-heat transfer density is the optimal spacings that have been reported for forced convection [3-6]. The progress in

this area has been reviewed in [1, 7]: Optimal spacings have been determined for parallel plate channels, cylinders in cross-flow, staggered parallel plates, and pin fin arrays with impinging flow. In each configuration, the optimal spacing is a single-length scale that is distributed throughout the available volume.

The optimal spacing idea was taken theoretically and numerically one step further in [8-10], where the flow structure had not one but several optimal-length scales. These were distributed non-uniformly through the flow space, more, numerous and smaller in the entrance region of the available volume. The reason is that the boundary layers were thinner and more plates could be fitted together optimally.

In this paper, we evaluated this design approach numerically, by considering forced convection cooling of a volume filled by stacks of three-dimensional parallel plates that generate heat. This represents the actual geometry in space and the limitation of the result obtained using two-dimensional parallel plates [8] is eliminated. The flow and heat transfer are simulated numerically for a wide variety of flow configurations. Each numerical simulation shows that the entrance region of every parallel plate channel has a core of unused (isothermal) fluid. In this wedge-shaped region, we progressively inserted smaller heat-generating plates, and then we optimised the multi-scale assembly. The maximisation of heat transfer density is pursued geometrically, by varying more and more degrees of freedom. The result is a class of progressively better flow structures with multiple-length scales that are distributed non-uniformly through the flow system.

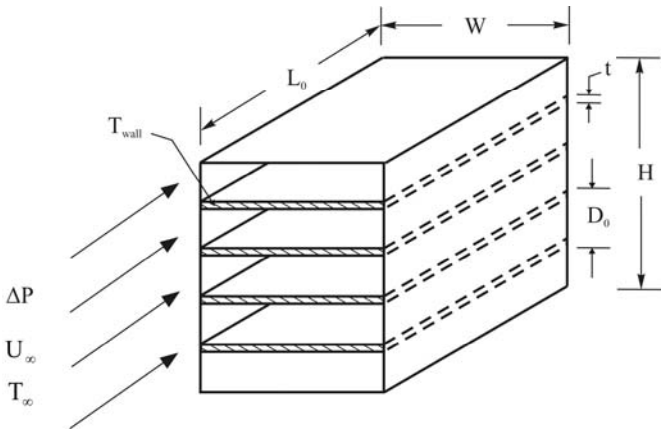

Figure 1 Three-dimensional stacks of parallel plate channels.

PHYSICAL MODEL

Consider a stack of three-dimensional heat-generating parallel plates in space as shown in Figure 1, the plates are modelled as isothermal with temperature $T = T_{wall}$. A stream of coolant with temperature $T = T_\infty$ is forced through the channels in a fixed volume. The problem consists of maximising the heat transfer rate between the coolant and the heat-generating plates.

The problem is ruled by the conservation of mass, momentum and energy equations. They are simplified in accordance with the assumptions of three-dimensional incompressible steady-state laminar flow with constant properties for a Newtonian flow. The governing equations in the dimensionless forms are:

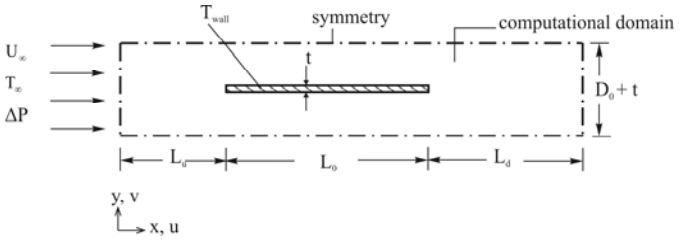

(2a)

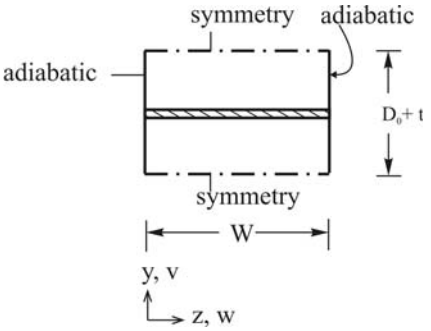

(2b)

Figure 2a,b Computational domains for a three-dimensional parallel plate channel.

$$\frac{\partial \tilde{u}}{\partial \tilde{x}} + \frac{\partial \tilde{v}}{\partial \tilde{y}} + \frac{\partial \tilde{w}}{\partial \tilde{z}} = 0 \qquad (1)$$

$$\frac{Be}{Pr}\left(\tilde{u}\frac{\partial \tilde{u}}{\partial \tilde{x}} + \tilde{v}\frac{\partial \tilde{u}}{\partial \tilde{y}} + \tilde{w}\frac{\partial \tilde{w}}{\partial \tilde{z}}\right) = -\frac{\partial \tilde{P}}{\partial \tilde{x}} + \nabla^2 \tilde{u} \qquad (2)$$

$$\frac{Be}{Pr}\left(\tilde{u}\frac{\partial \tilde{v}}{\partial \tilde{x}} + \tilde{v}\frac{\partial \tilde{v}}{\partial \tilde{y}} + \tilde{w}\frac{\partial \tilde{v}}{\partial \tilde{z}}\right) = -\frac{\partial \tilde{P}}{\partial \tilde{y}} + \nabla^2 \tilde{v} \qquad (3)$$

$$\frac{Be}{Pr}\left(\tilde{u}\frac{\partial \tilde{w}}{\partial \tilde{x}} + \tilde{v}\frac{\partial \tilde{w}}{\partial \tilde{y}} + \tilde{w}\frac{\partial \tilde{w}}{\partial \tilde{z}}\right) = -\frac{d\tilde{P}}{d\tilde{z}} + \nabla^2 \tilde{w} \qquad (4)$$

$$Be\left(\tilde{u}\frac{\partial \tilde{T}}{\partial \tilde{x}} + \tilde{v}\frac{\partial \tilde{T}}{\partial \tilde{y}} + \tilde{w}\frac{\partial \tilde{T}}{\partial \tilde{z}}\right) = \nabla^2 \tilde{T} \qquad (5)$$

Where $\nabla^2 = \partial^2/\partial\tilde{x}^2 + \partial^2/\partial\tilde{y}^2 + \partial^2/\partial\tilde{z}^2$, and the variables are defined as,

$$\tilde{x},\tilde{y},\tilde{z} = \frac{(x,y,z)}{L_0}, \qquad \tilde{P} = \frac{P}{\Delta P} \qquad (6)$$

$$(\tilde{u},\tilde{v},\tilde{w}) = \frac{(u,v,w)}{\Delta P L_0/\mu}, \qquad \tilde{T} = \frac{T-T_\infty}{T_w - T_\infty}$$

$$Be = \frac{\Delta P\, L_0^2}{\alpha\mu}, \qquad Pr = \frac{\nu}{\alpha}$$

(7)

In Eq. (7), Be is the dimensionless pressure drop number [11], and Pr the Prandtl number. There is no flow in the fraction of the volume occupied by the solid plates and, therefore, only the energy equations need to be solved in the portion occupied by the plates, $\nabla^2\tilde{T} = 0$.

Symmetry allowed us to reduce the computational domain to a unit cell, which is represented by the computational domain shown in Fig. 2a and 2b. The computational domain is composed of external fluid and a solid heated plate. The fluid flows through the channels as well as the frontal area of the plates in the direction of the flow. The three-dimensional parallel plates are arranged equidistantly from one another, and the thickness of the plate is assumed to be the same for all the plates. To complete the problem formulation, the following boundary conditions are then specified for the extended three-dimensional computational domain in line with Fig 2a and 2b:

$$\tilde{P}=1, \quad \tilde{v} = \tilde{w} = 0, \quad \tilde{T} = 0 \text{ at } \tilde{x} = 0 \tag{8}$$

$$\tilde{u} = \tilde{v} = \tilde{w} = \frac{\partial \tilde{T}}{\partial \tilde{z}} = 0, \text{ at } \tilde{z} = 0 \text{ and } \tilde{z} = \tilde{W} \tag{9}$$

$$\frac{\partial \tilde{u}}{\partial \tilde{y}} = \frac{\partial \tilde{w}}{\partial \tilde{y}} = v = 0 \quad \text{at } \tilde{y} = 0 \text{ and } \tilde{y} = \tilde{D}_0 + t \tag{10}$$

$$\tilde{u} = \tilde{v} = \tilde{w} = 0, \quad \tilde{T} = 1 \quad \text{at the surface of the plates} \tag{11}$$

$$\tilde{P} = \frac{\partial \tilde{u}}{\partial \tilde{x}} = \frac{\partial \tilde{v}}{\partial \tilde{x}} = \frac{\partial \tilde{w}}{\partial \tilde{x}} = \frac{\partial \tilde{T}}{\partial \tilde{x}} = 0 \quad \text{at } \tilde{x} = (\tilde{L}_0 + \tilde{L}_u + \tilde{L}_d) \tag{12}$$

Additional boundary conditions are zero shear and zero heat flux around the periphery of the computational domain and no-slip on the plate surfaces in contact with the fluids. It should be noted that the numerical task of simulating the flow and temperature fields in stacks cooled by a free stream in three dimensions is considerable and more time-consuming than when the stacks are sandwiched between two parallel plates or are in two dimensions. In the latter, there is no coolant bypass around the stack by a free stream and it is sufficient to perform calculations only for one plate-to-plate channel. In order to represent the actual flow, an extension was added to the computational domains. The extent of the computational domains ($\tilde{L}_u$ and $\tilde{L}_d$) was chosen such that the flow behaves like a free stream (i.e. is not affected by the stacks in regions situated sufficiently far from the stack), see Fig. 2. The upstream reservoir frees the flow and allows it to develop hydraulically starting at the entrance plane of the channel, while the uniform inlet flow boundary condition is specified at the entrance plane of the upstream reservoir. Doing this, eliminates the need to impose a velocity profile at the entrance of the channels. The downstream reservoir of the computational domain delayed the imposition of an unrealistic outlet boundary condition on the exit plane of the channel. The symmetry about $\tilde{y} = 0$ and $\tilde{y} = \tilde{D}_0 + \tilde{t}$, allowed us to perform the calculations in the region defined by Fig. 1b of the field, namely ($0 \le \tilde{y} \le \tilde{D}_0 + \tilde{t}$). The temperature profile in the volume occupied by the plates is solved simultaneously with Eqs. (1)-(5) for the fluid portion of the domain.

The global objectives of this study are to find the optimal geometry such that the volumetric heat transfer rate density is maximised. The dimensionless heat transfer rate density is defined as follows:

$$\tilde{q} = \frac{q}{k(T_w - T_\infty)D_0} \tag{13}$$

Where the overall heat transfer rate between the parallel plates and free stream, q, has been divided by the constrained volume L_0HW, *k* is the fluid thermal conductivity.

NUMERICAL METHOD

In this work, we used the finite volume code (FLUENT^{TM}) to solve the continuity, momentum and energy equations. A detailed discussion of the finite volume method is available in Patankar [12]. The second-order upwind scheme was used to model the combined convection-diffusion effect in the transport equations. Convergence is obtained when the residuals for the mass and momentum equation are smaller than 10^{-4}, and the residual of the energy equation becomes less than 10^{-9}. To obtain accurate numerical results, several mesh/grid refinement tests were conducted. The monitored quantity was overall heat transfer rate density, computed with Eq. (13), according to the following criterion:

$$\gamma = \left|\tilde{q}_j - \tilde{q}_{j-1}\right| \Big/ \left|\tilde{q}_j\right| \le 0.02 \tag{14}$$

where j is the mesh iteration index, such that j increases when the mesh is more refined. When the criterion is satisfied, the j-1 mesh is selected as the converged mesh. The above criterion was also extended to find the appropriate lengths ($\tilde{L}_u$, $\tilde{L}_d$) for the computational domain and γ was set ≤ 0.001. Using the above criterion, the test showed that the size of the computational domain ($L_u = 2L_0$ and $L_d = 3L_0$) is large enough, so that the total heat rate, $\tilde{q}$ (with changes less than 1 %), is insensitive to further increase in $\tilde{L}_u$ and $\tilde{L}_d$. These tests were conducted for Be = 10^5 and 10^7.

OPTIMAL SPACING FOR STACK OF THREE-DIMENSIONAL PLATES

In the first phase of this study, we simulated numerically the heat and fluid flow fields for the systems in Fig. 2a and 2b in the laminar range represented by $10^5 \le$ Be $\le 10^7$, plate thickness $0.01 \le \tilde{t} \le 0.05$ and width $\tilde{W} = 1$, for several geometries in search of optimal spacing. The optimisation of the stack of parallel plate channels has one degree of freedom, the spacing between the plates. This was optimised for a given Be and Pr and a fixed plate thickness. Fig. 3a shows the result of optimising a stack of three-dimensional parallel plate channels cooled with a free stream. Figure 3a also shows that there exists an optimal spacing for three-dimensional parallel plate channels with isothermal temperatures.

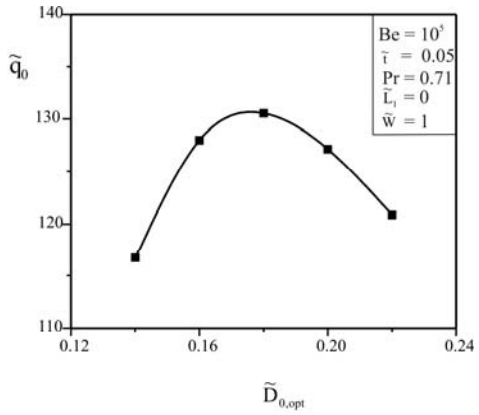

Figure 3a Numerical optimisation result for parallel plate channel spacing.

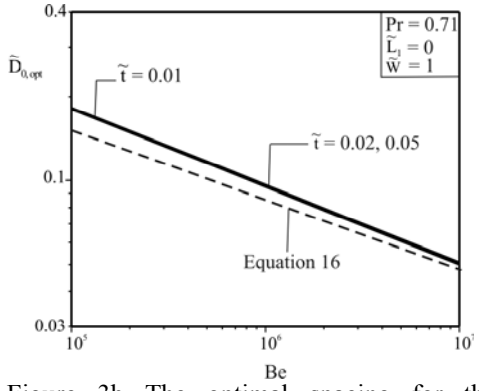

Figure 3b The optimal spacing for three-dimensional parallel plates with finite thickness.

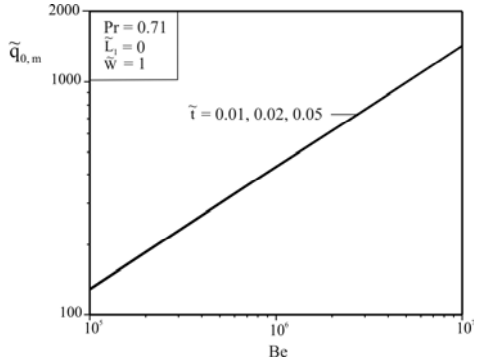

Figure 3c The maximised total heat transfer rate that corresponds with a three-dimensional plate with finite thickness.

Figure 3b summarises the relationship between the optimal spacing in the range of assumed parameters given above. And it shows that as the dimensionless pressure number increases, the optimal spacing decreases. The effect of plate thickness is negligible. This is due to the fact that the scales of the length and width of the plate are much greater than the plate thickness. To further validate our numerical result, we compare our results with the one obtained by Bejan and Scuibba [3] in their study of cooling a stack of parallel plates with an imposed pressure difference ΔP between x = 0 and x = L_0. In that study, the plate-to-plate channel flow was identical, because the stack cooled was in a two-dimensional channel formed between two adiabatic plates with the distance H in between them (no three-dimensional effect and no free stream around the stack). It was further assumed that the plate thickness is negligible, and that the plate-to-plate spacing, d is small when compared with H or that the number of plates is large

$$n = \frac{H}{d} >> 1 \qquad (15)$$

The analysis produced the following optimal for a stack with uniform temperature on both sides of each plate;

$$\frac{d_{opt}}{L_0} \cong 2.7 Be_{L_0}^{-1/4} \qquad (Pr \geq 0.71) \qquad (16)$$

From Fig. 3b, the optimal spacing in the log-log graphs of Fig. 3b for $\tilde{\tau} = 0.01$ can be correlated with the expressions

$$\tilde{D}_{0,opt} \cong 4.51 Be^{-0.28} \qquad (\tilde{\tau} = 0.01, Pr = 0.71) \qquad (17)$$

Figure 3c summarises the effect of the dimensionless pressure drop number and plate thickness on the maximum heat transfer. As Be increases, the maximum heat transfer rate from the plates also increases. The effect of plate thickness, $\tilde{\tau}$ on the heat transfer rate density is negligible. The maximum heat transfer rate density in the log-log graphs of Fig. 3c for $\tilde{\tau} = 0.05$ can be correlated with the expressions

$$\tilde{q}_{max} \cong 0.31 Be^{0.522} \quad (\tilde{\tau} = 0.05) \qquad (18)$$

These results are in agreement with the constructal method (Ref [1], chapter 3, Ref [9]) according to which the maximal heat transfer means 'optimal packing' such that flow regions that do not contribute to global performance are eliminated. This implies that the packing of Fig. 1 is achieved when the three-dimensional plates are brought close enough such that their thermal boundary layers just touch. The thermal boundary layer of a parallel plate with laminar flow and fluid Prandtl number of order 1 and length L_0, has a thickness of order

$$\delta_T \cong 0.5 L_0 \, Re_{L_0}^{-1/2} \qquad (19)$$

The behaviour of equations (17, 18, 19) suggests that the structure of Fig. 1 can be improved further if we insert shorter plates midway (see Ref [9]) at the entrance of the three-dimensional plate channels. These possibilities will be discussed in the next section.

THREE-DIMENSIONAL PARALLEL PLATES WITH SMALL PLATE INSERT

In the sequence of increasing more complex structures and utilising the fluid wedge between two parallel plates, we inserted smaller plates; we inserted a small $\tilde{L}_1$-long plate as shown in Figs. 4 and 5. Using the same procedure outlined above, we numerically solved the governing equations 1-5, subject to the same boundary conditions.

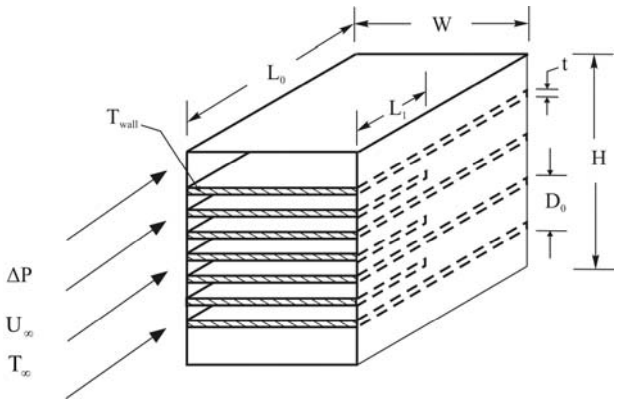

Figure 4 Three-dimensional stacks of parallel plates, with smaller plate insert.

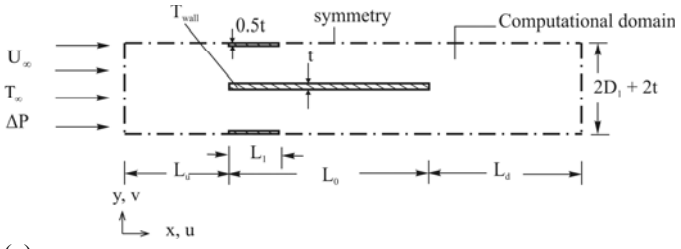

(a)

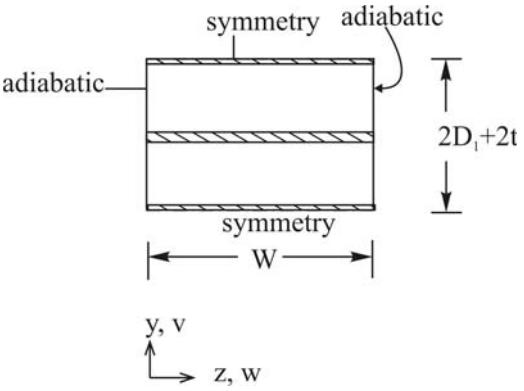

(b)

Figure 5(a, b) Computational domain for a three-dimensional parallel plate channel, with short plate inserts.

To determine the contribution of the $\tilde{L}_1$-long plate, we fixed $\tilde{D}_{0,\,opt}$ at the values determined previously (Fig. 3) so that the already optimised structure stays the same. The spacing between L spacing becomes $\tilde{D}_{opt} = 2\,\tilde{D}_{1,opt}$. The thickness of the 3-D plates was set at $\tilde{t} = 0.05$, as the maximised $\tilde{q}$ is insensitive to changes in $\tilde{t}$ as previously determined. We now optimized $\tilde{L}_1$ by varying its length until we obtained an optimal length that corresponded to the new maximised $\tilde{q}$, this is reported in Figure 6a. The procedure stated above was repeated for several Be in the range $10^5 \le Be \le 10^7$ and Pr = 0.71. Note the ratio of $\tilde{D}_{0,opt} / \tilde{D}_{1,opt} = 2$. Fig. 6a shows the behaviour of the optimal-length scale, $\tilde{L}_{1,opt}$. The optimal-length scale increases as the dimensionless pressure drop number increases. The results are in agreement with [8], which shows that as the Be increases, the optimal plate insert also increases.

Figure 6c shows the effects of Be on the maximal heat transfer rate density for the two combinations of length scales. The maximal heat transfer rate density increases as the number of plates increases. It is expected that this would become less noticeable as the number of length scales increases, hence for this work the number of plate inserts was limited to one.

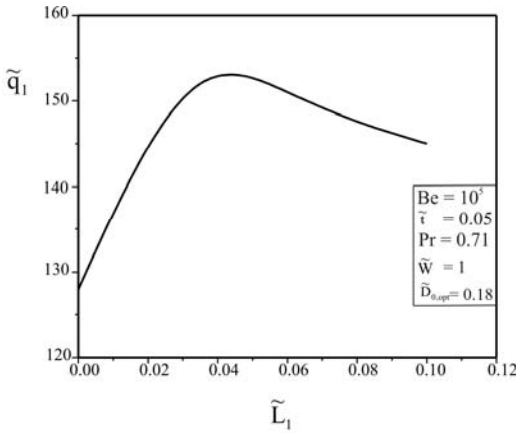

Fig.6a The effect of the length $\tilde{L}_1$ on the dimensionless total heat transfer density.

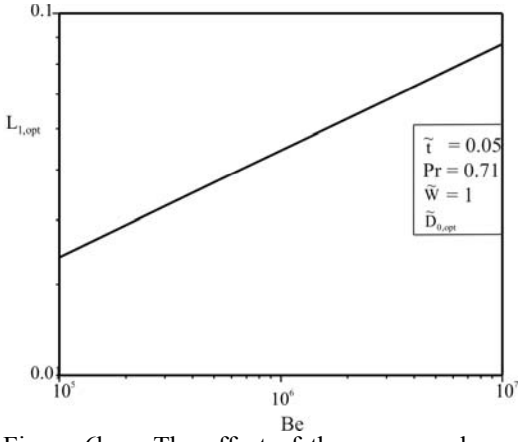

Figure 6b The effect of the pressure drop number on the optimised length scale.

Figure 6c also shows that the maximised heat transfer rate density increases in proportion to $Be^{1/2}$. This confirms the analytical result [9], which can be rewritten in the notation employed in this paper:

$$\tilde{q} = 0.36 Be^{1/2}\left(1+\frac{m}{2}\right)^{1/2} \qquad (20)$$

Parameter m is the number of new (inserted) plate lengths, for example when m = 1 as in Figure 6c. The prediction (20) is that the heat transfer rate density increases in progressively

smaller steps as the number of length scales increases. This is confirmed by the numerical result shown in Fig. 6c.

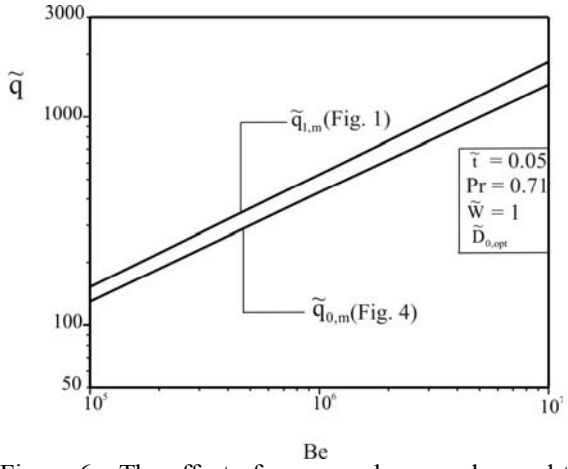

Figure 6c. The effect of pressure drop number and the number of length scales on the dimensionless maximum total heat transfer density.

Table 1 shows that the numerical result confirms the theoretical predictions of Bejan and Fautrelle, which show an increase of 19% in heat transfer rate density. This compares favourably with the increase of 22% obtained from the theoretical work of Bejan and Fautrelle.

Table 1. Comparison between the numerical and analytical results for the maximised heat transfer rate density of the multi-scale flow construct.

m	Analytical [9]	$\tilde{q} / Be^{1/2}$ Numerical Result (Figure 6c)
0	0.36	0.431
1	0.44	0.529
% increase	22	19

CONCLUSIONS

In this paper, we illustrated the emergence of a multi-scale forced convection flow structure for maximal heat transfer rate density for three-dimensional parallel plates installed in a fixed volume. This objective was achieved by inserting smaller plates in the entrance region formed between successive plates. This technique utilises to the fullest the fluid surrounding the two tips of two neighbourhood plates where the boundary layers are the thinnest, the optimised spacings were fixed with each new (smaller) plate that is inserted in the entrance region of each channel.

As the number of plates increases, it is expected that the flow structure becomes less permeable and the flow rate decreases. At the same time, the total heat transfer rate density from the solid structure increases. It was found numerically that when the number of plates increases to three, the increase in the heat transfer rate density becomes less noticeable [8], hence for this numerical computation the number of plates inserted in the flow structure was limited to one.

Optimal spacings were found numerically for structures with one length scale. Performance increases as complexity increases, that is the new plates are inserted into the structures. The number of plate-length scales is limited by the validity of the boundary layer assumption. The smallest plate is the one where the plate length is comparable with the boundary layer thickness.

The fundamental value of this study is that multi-scale flow structures are applicable to every sector of heat exchanger design. The novelty is the increase in heat transfer density, and the non-uniform distribution of length scales through the available space. This approach promises the development of new and unconventional internal flow structures for heat exchangers and cooled electronic packages.

REFERENCES

[1] Bejan, A., Shape and Structure, from Engineering to Nature, Cambridge University Press, Cambridge, UK, 2000.

[2] Dirker, J., Van Wyk, J. D. and Meyer, J. P., Cooling of Power Electronics by embedded solids, Journal of Electronic Packaging, Vol. 128, 2006, pp. 388 – 397.

[3] Bejan, A., and Sciubba, E., The optimal spacing for parallel plates cooled by forced convection, *International Journal of Heat and Mass Transfer*, Vol. 35, 1992, pp. 3259-3264.

[4] Morega, A. M., Bejan, A. and Lee, S. W., Free stream cooling of a stack of parallel plates, *International Journal of Heat and Mass Transfer*, Vol. 38, 1995, pp. 519 – 531.

[5] Koo, J.-M., Im, S., Jiang, L., and Goodson, K. E., Integrated microchannel cooling for three-dimensional electronic architectures, *Journal of Heat Transfer*, Vol. 127, 2005, pp. 49- 58.

[6] Matos, R. S., Laursen, T. A., Vargas, J. V. C. and Bejan, A., Three-dimensional optimization of staggered finned circular and elliptic tubes in forced convection, *International Journal of Thermal Sciences*, Vol. 43, 2004, pp. 447 – 487.

[7] Kim, S. J., and Lee, S. W., eds., Air Cooling Technology for Electronic Equipment, CRC Press, Boca Raton, FL, 1996, Chapter 1.

[8] Bello-Ochende, T. and Bejan, A., Maximal heat transfer density: Plates with multiple lengths in forced convection, *International Journal of Thermal Sciences*, Vol. 43, 2004, pp. 1181 – 1186.

[9] Bejan, A. and Fautrelle, Y., Constructal multi-scale structure for maximal heat transfer density, *Acta Mechanica*, Vol. 163, 2003, pp. 39-49.

[10] Da Silva, A. K. and Bejan A., Constructal multi-scale structure for maximal heat transfer density in natural convection, *International Journal of Heat and Fluid Flow*, Vol. 26, 2005, pp. 34- 44.

[11] Petrescu, S., Comments on the optimal spacing of parallel plates cooled by forced convection, *International Journal of Heat and Mass Transfer*, Vol. 37, 1994, pp. 1283.

[12] Patankar, S. V., Numerical Heat Transfer and Fluid flow, Hemisphere, Washington DC, 1980.